



HAL
open science

Plasma codeposition of transparent thin films : relationship between the surface chemistry and the anti-fogging property

Thanh Hien Tran, Dominique Debarnot, Jose Ortiz, Fabienne
Poncin-Epaillard

► To cite this version:

Thanh Hien Tran, Dominique Debarnot, Jose Ortiz, Fabienne Poncin-Epaillard. Plasma codeposition of transparent thin films : relationship between the surface chemistry and the anti-fogging property. *Plasma Processes and Polymers*, 2019, 16 (10), pp.1900070. 10.1002/ppap.201900070 . hal-03367767

HAL Id: hal-03367767

<https://hal.science/hal-03367767v1>

Submitted on 6 Oct 2021

HAL is a multi-disciplinary open access archive for the deposit and dissemination of scientific research documents, whether they are published or not. The documents may come from teaching and research institutions in France or abroad, or from public or private research centers.

L'archive ouverte pluridisciplinaire **HAL**, est destinée au dépôt et à la diffusion de documents scientifiques de niveau recherche, publiés ou non, émanant des établissements d'enseignement et de recherche français ou étrangers, des laboratoires publics ou privés.

Plasma codeposition of transparent thin films : relationship between the surface chemistry and the anti-fogging property.

Thanh Hien Tran^{a)}, Dominique Debarnot^{a)}, Jose Ortiz^{b)}, Fabienne Poncin-Epaillard^{a)*}

Dr T. H. Tran, Dr D. Debarnot, Dr F. Poncin-Epaillard
Institut des Molécules et Matériaux du Mans (IMMM) - UMR 6283 CNRS, Le Mans,
Université, Avenue Olivier Messiaen, 72085 Le Mans Cedex 9, France
E-mail: Fabienne.Poncin-Epaillard@univ-lemans.fr
J. Ortiz
VIS - Lighting Headquarters - 34 rue Saint André, 93000 Bobigny, France

Plasma Proc. Polym., 16(10), e1900070 (2019)

Anti-fogging coatings are deposited on the polycarbonate thanks to the low pressure pulsed plasma. Two precursors are simultaneously polymerized : one contains hydrophilic groups (2-(dimethylamino)ethyl methacrylate or acrylic acid) while the other one (1H,1H,2H-perfluoro-1-decene) is hydrophobic. Several proportions of (1H,1H,2H-perfluoro-1-decene) are applied in order to prepare films with high hexadecane ($\approx 70^\circ$) and low water ($\leq 20^\circ$) contact angles. Evidence of their hydrophilic, oleophobic properties is given by the wettability and the anti-fogging measurements. It appears that all plasma-codeposits issued from acrylic acid and 1H,1H,2H-perfluoro-1-decene with high HCA are more oleophobic than the plasma-copolymers 2-(dimethylamino)ethyl methacrylate and 1H,1H,2H-perfluoro-1-decene, irrespective of the proportion of the fluorinated precursor. Such a behavior is explained by the grafting of longer perfluorinated chains. The anti-fogging properties are not directly correlated to the wettability. Moreover, the films act as predicted by the flip flop mechanism.

Key words: plasma deposition ; hydrophilic / oleophobic coating ; anti-fogging ; wetting.

1 Introduction

Anti-fogging coating a polymeric substrate has been investigated in recent years since the fog observed on eyeglasses, goggles, camera lens, and automobile windows damaged the optical properties (i.e. the transparency) of many products. ^[1-3] The fog occurs when the water vapor condenses on the surface and forms discrete dispersed water particles, fairly broad to scatter the light, thereby restricting the light transmission and the optical efficiency. For preventing the fog appearance, the transition from water droplets to the uniform water film must be enhanced as described for the solid surface showing a critical water contact angle (WCA) smaller than 40 °. ^[4,5] Generally, hydrophilic properties and the consequent water monolayer formation are reached thanks to synthetic polymers bearing either hydroxyl (OH), carboxyl (COOH, COOR), amino (NH_x) or sulfonic (SO₃H) groups often layered on a substrate by dip-coating, spin-coating method. ^[3,6-10] Another anti-fogging method involves nanostructured coatings prepared by the wet etching of oxide films such as silica and titanium oxide or by the plasma treatment of polymer films. ^[11-14]

Such a hydrophilic surface may age at ambient atmosphere followed by the reduction of its anti-fogging property. The ageing of hydrophilic surfaces was assigned to the adsorption of organic air-borne contaminants. ^[15,16] Thus, in order to reduce the hydrocarbon contamination, the combination of hydrophilic - oleophobic properties appears to be a promising framework for preparing a long-term anti-fogging surface. In addition to a WCA ≤ 40°, such a surface must then present a hexadecane contact angle (HCA) around 70 °. The high HCA is expected to repel any oil or organic contaminant and thus, to preserve the antifogging property. Therefore, such a surface must be composed of hydrophilic dangling groups or chain segments and hydrophobic / oleophobic counterpart. Indeed, Wang *et al* demonstrated that, after 14 days, a perfluoropolyether (HOCH₂CF₂O-[CF₂CF₂O]_m-[CF₂O]_n-CF₂CH₂OH) coating showing a WCA

= $46.5 \pm 0.9^\circ$ and a HCA = $70.1 \pm 0.9^\circ$ presents improved anti-fogging performance compared to the corresponding hydrophilic and oleophilic coating ($\text{CH}_3\text{CF}_2\text{O}-[\text{CF}_2\text{CF}_2\text{O}]_m-[\text{CF}_2\text{O}]_n-\text{CF}_2\text{CF}_3$) with WCA = $43.4 \pm 0.8^\circ$ and HCA = $32.6 \pm 0.5^\circ$.^[17]

Two possible anti-fogging mechanisms of hydrophilic - oleophobic surface behavior have been proposed.^[4,17-19] The first one, so-called “penetration” mechanism relies on the difference in the kinetics of absorption between the diffusing molecules (water or hexadecane) depending on their respective sizes, through the rearrangement of hydrophobic chains at the upper layer. The higher the molecule size is, the slower the penetration is and the higher the contact angle value is.^[17,20] Thus, a HCA higher than WCA is expected. The second mechanism, so-called “flip-flop” mechanism proposed by H. Sawada *et al.*^[19] is based on the turn-over of the hydrophobic or hydrophilic segments inside the material and in an opposite manner, the reorientation at the surface of hydrophilic or hydrophobic chains according to the liquid nature (hexadecane or water) respectively.

Several methods were proposed for preparing these hydrophilic - oleophobic surfaces such as dip-coating^[21], spin-coating^[4], spraying^[22] of different types of inorganic and / or organic materials. For example, the hydrophilic and oleophobic surface can be prepared by dip-coating a plasma polymerized (p) acrylic acid substrate with an ionic amphiphilic fluoro-surfactant.^[21] Another illustration is given with a silica substrate modified by the isocyanate-silane then covalently grafted with perfluorinated polyethylene glycol oligomers leading to HCA = 67° higher than WCA (= 30°).^[4]

In this work, we explore the plasma polymerization, a more environmental friendly technique for preparing such hydrophilic - oleophobic surfaces. Two types of precursors were chosen in function of their hydrophilicity, such as 2-(dimethylamino)ethyl methacrylate (DAME) or acrylic acid (AA), and their hydrophobicity, such as 1H,1H,2H-perfluoro-1-decene (HDFD) in order to prepare two plasma co-deposited films : p-DAME-co-HDFD and p-AA-co-HDFD. The influence of the HDFD proportion on the bulk and the surface chemical

structures, the wettability of the obtained layer is studied. The anti-fogging property of such co-deposits is demonstrated thanks to the water vapor contact test and the transmittance measures. The proportions of hydrophilic and hydrophobic segments and the perfluorocarbon-chains rearrangement for each plasma co-deposited film are discussed in function of the anti-fogging performance.

2 Experimental Section

2.1 Elaboration of p-DAME-co-HDFD and p-AA-co-HDFD thin layers

2-(dimethylamino) ethyl methacrylate (DAME, $\text{CH}_2=\text{C}(\text{CH}_3)\text{COOCH}_2\text{CH}_2\text{N}(\text{CH}_3)_2$, Acros Organics, France, 99 % purity), acrylic acid (AA, $\text{CH}_2=\text{CHCOOH}$, Sigma Aldrich France, 99 % purity) and 1H,1H,2H-perfluoro-1-decene (HDFD, $\text{CF}_3(\text{CH}_2)_7\text{CH}=\text{CH}_2$, Sigma Aldrich France, 99 % purity) were used as received.

Coatings were directly deposited on polycarbonate (PC) substrates for the wettability measurement, on Si/SiO₂ wafer for the XPS spectroscopy and on pressed KBr pellets for the FTIR spectroscopy.

The used RF (13.56 MHz) plasma reactor corresponds to a capacitive coupling system (MG300S, Plassys) made of cylindrical aluminum chamber (28 cm diameter and 6.15 L volume) with two parallel circular electrodes (20 cm diameter with a 9.5 cm gap). The substrates were located on the lower cathode. Before any deposition, the PC surface was pre-treated by Ar plasma for a higher adhesion (flow : $F_{Ar} = 10$ sccm, discharge power : $P = 100$ W, duration : $t = 30$ s). Then, the precursor vapors (DAME or AA, HDFD) were together injected through an electrode-integrated shower. The pressure was measured by a capacitive gauge (Baratron, Leybold). In the case of the copolymerization, the first precursor was injected until its required partial pressure, then the second one was added as follows the desired ratio. Partial pressure of

each gas was determined as the difference of total pressure before and after introduction. The total pressure was maintained constant at 0.02 Torr during the overall polymerization process.

p-DAME-co-HDFD and p-AA-co-HDFD were deposited, with different HDFD concentrations in the mixture, using the pulsed plasma technique with the following plasma parameters : discharge power $P = 10$ W, deposition time $t = 10$ min, pulse on-time (t_{on}) = 17 μ s, pulse off-time (t_{off}) = 150 μ s, leading to an applied frequency $f = 6$ kHz for a duty cycle $d.c.$ (defined as the ratio of pulse on-time to period) = 10 %. The parameters domains were selected in order to obtain a transparent plasma codeposit. More drastic plasma conditions (i.e. more important fragmentation of the precursors) led to yellow deposited layers.

2.2 Film characterization

2.2.1 FTIR spectroscopy

Chemical composition of the p-DAME-co-HDFD and p-AA-co-HDFD deposited on transparent KBr pellets was extracted from Bruker Vertex 70v spectrometer with 2 cm^{-1} resolution in the range 4000 - 400 cm^{-1} , 20 scans were recorded. The FTIR spectra were done 10 min after the sample deposition. Spectral data were treated with Opus software for baseline correction and CO_2 / H_2O subtraction. All the spectra intensities were normalized by the thickness of each co-deposited layer.

2.2.2 Wettability

The wettability of the plasma layers on PC substrate was carried out thanks a goniometer with 3 μ l high purity water drops (MilliQ Water System, resistivity 18 $\text{M}\Omega \text{ cm}^{-1}$) and n-hexadecane drops ($\text{CH}_3(\text{CH}_2)_{14}\text{CH}_3$, Sigma-Aldrich France, ≥ 99 %). Measurements were run

on both sides of the drop and were averaged of five experiments with a standard deviation comprised between 0.8 and 1.7 °.

2.2.3 X-Ray Photoelectron Spectroscopy (XPS)

The plasma co-deposits on PC film were analyzed by XPS instrument (Kratos Axis Nova, UK) located at the Institut des Matériaux de Nantes (France) with a the monochromatic Al K α beam at the electron emission angle of 90 ° relative to the sample surface. The pass energies for survey spectra were 80 eV (increment = 0.5 eV) and 20 eV (increment = 0.1 eV) for high resolution. The full width at half-maximum (FWHM) for the Gaussian peaks was maintained as a constant value for all atomic components, but depending on the layer type, it varied from 1.4 to 1.8 eV. The high resolution fitting accuracy was 5 %.

2.2.4 Layer thickness measurement

The thickness measure of the different layers deposited on Si/SiO₂ wafer was performed thanks to AFM machine (Bruker Innova). Before the deposition, the substrate is partially masked. After the plasma process, the mask was removed and the levels difference corresponds to the thickness of the deposit. 50 x 50 μm^2 areas were scanned in tapping mode at ambient air. The film thicknesses were determined using Gwyddion software and were presented in **Table 1** for all the synthesized films.

Table 1. Film thickness of p-DAME-co-HDFD and p-AA-co-HDFD with different HDFD proportions (%).

| [HDFD] (%) | Film thickness (nm) | |
|---------------|---------------------|------------------|
| | p-DAME-co-HDFD | p-AA-co-HDFD |
| 0 | 27.9 \pm 1.8 | 101.9 \pm 20.7 |
| 10 | 58.2 \pm 10.9 | 68.4 \pm 13.0 |
| 20 | 37.7 \pm 5.8 | 38.6 \pm 6.7 |

| | | |
|-----|----------------|----------------|
| 50 | 14.2 ± 2.6 | 15.6 ± 2.3 |
| 100 | 13.8 ± 2.4 | 13.8 ± 2.4 |

2.2.5 Anti-fogging procedure

The anti-fogging properties of thin films were checked from a protocol derived from the ISO standard EN 168. The sample was exposed to the water vapor during 1 min at 5 cm from the liquid phase heated at 60 °C; then the transmittance (T) of the film was followed at $\lambda = 550$ nm by using UV-Visible spectrophotometer (Varian Cary 100 Scan).

3 Results and Discussion

3.1 Influence of the plasma chemistry on the chemical structure of plasma co-deposited films

Our approach for the elaboration of the anti-fogging coating is based on the synthesis of hydrophilic - oleophobic surface on PC substrate by plasma co-deposition. Therefore, the plasma phase is composed of a mixture of the hydrophilic monomer (AA or DAME containing either carboxylic groups ($-\text{COOH}$) or tertiary amino ($-\text{CH}_2\text{N}(\text{CH}_3)_2$) groups) and the fluorinated precursor (HDFD).

The composition and hydrophilic / hydrophobic properties of the coatings are linked to the proportion of monomers in the plasma mixture. Therefore, different p-DAME-co-HDFD and p-AA-co-HDFD are deposited at fixed plasma parameters ($P = 10\text{W}$, $f = 6\text{ kHz}$, $d.c. = 10\%$, $t = 10\text{ min}$) while varying the HDFD proportion. Indeed, the plasma chemistry is driven by the density and the energy of the different plasma species (precursor fragments, radicals, ions, electrons...) that offer a wide variety of plasma processes. However, only few of these lead to transparent deposit on PC as film prepared in such conditions : $P = 10 - 30\text{ W}$, $f = 6\text{ kHz}$, $d.c. =$

10 - 50 % ($t_{on} + t_{off} = 167 \mu s$). These so-called soft conditions induce less fragmentation, less deposited energy and allow the polymer growth during the plasma extinction as described in our previous paper. [23]

Figure 1 shows the FTIR spectra of p-DAME-co-HDFD and p-AA-co-HDFD versus the HDFD concentration in the plasma mixture. Note that the value of 0 % corresponds to DAME or AA homopolymers whereas the value of 100 % is associated to p-HDFD. The main vibration features of the different FTIR spectra of the homopolymers are identified :

- for the fluorinated layer : stretching of aliphatic CH_2 , CH_3 at $3028-2770 \text{ cm}^{-1}$, $CF=CF$ at 1645 cm^{-1} , $C-O/CF_3$ at 1260 cm^{-1} , CF_2 $1237 / 1155 \text{ cm}^{-1}$, $C-C$ 1208 cm^{-1} , bending of CF 1208 cm^{-1} , CF_2 $660-570 \text{ cm}^{-1}$. Hydroxyl groups are also identified with the vibration mode at $3500-3200 \text{ cm}^{-1}$ due to a possible post-oxidation ;

- for the acrylic layers : stretching of OH or NH at $3500-3200 \text{ cm}^{-1}$, aliphatic CH_2 , CH_3 at $3028 - 2770 \text{ cm}^{-1}$, $C=O$ at 1726 cm^{-1} . AA layer spectra also present stretching vibration bands as $(O=C)-OH$ at 1450 cm^{-1} , $C-O/C-O-C$ at $1412/1384 \text{ cm}^{-1}$ and aliphatic long-chain carboxylic acid at $1237 - 1183 \text{ cm}^{-1}$ while the spectra of the amido-acrylate layers reveal the presence of stretching bands of $C-N$ (tertiary) at $1263/1153 \text{ cm}^{-1}$, $C-O$ stretch at 1260 cm^{-1} and saturated $C-O-C$ at 1026 cm^{-1} .

Co-deposited coatings present a strong absorption band at $1370 - 1150 \text{ cm}^{-1}$ which is assigned to νCF_3 and $\nu C-C$ of HDFD monomer. In the case of p-DAME-co-HDFD layers, two other weak peaks at 1263 and 1153 cm^{-1} are assigned to $\nu C-N$ of tertiary aliphatic amines. Moreover, νCH_x vibration is represented by several bands at $2700 - 3000 \text{ cm}^{-1}$. Besides, the FTIR spectra of the p-AA-co-HDFD film show bands at 1726 cm^{-1} and $3500 - 3200 \text{ cm}^{-1}$ respectively assigned to $\nu C=O$ and νOH vibrations produced by precursor fragmentation during the plasma deposition or the post-oxidation after the film elaboration. This FTIR study has then shown that the two kinds of coatings present the characteristic bands of the two monomers in the mixture.

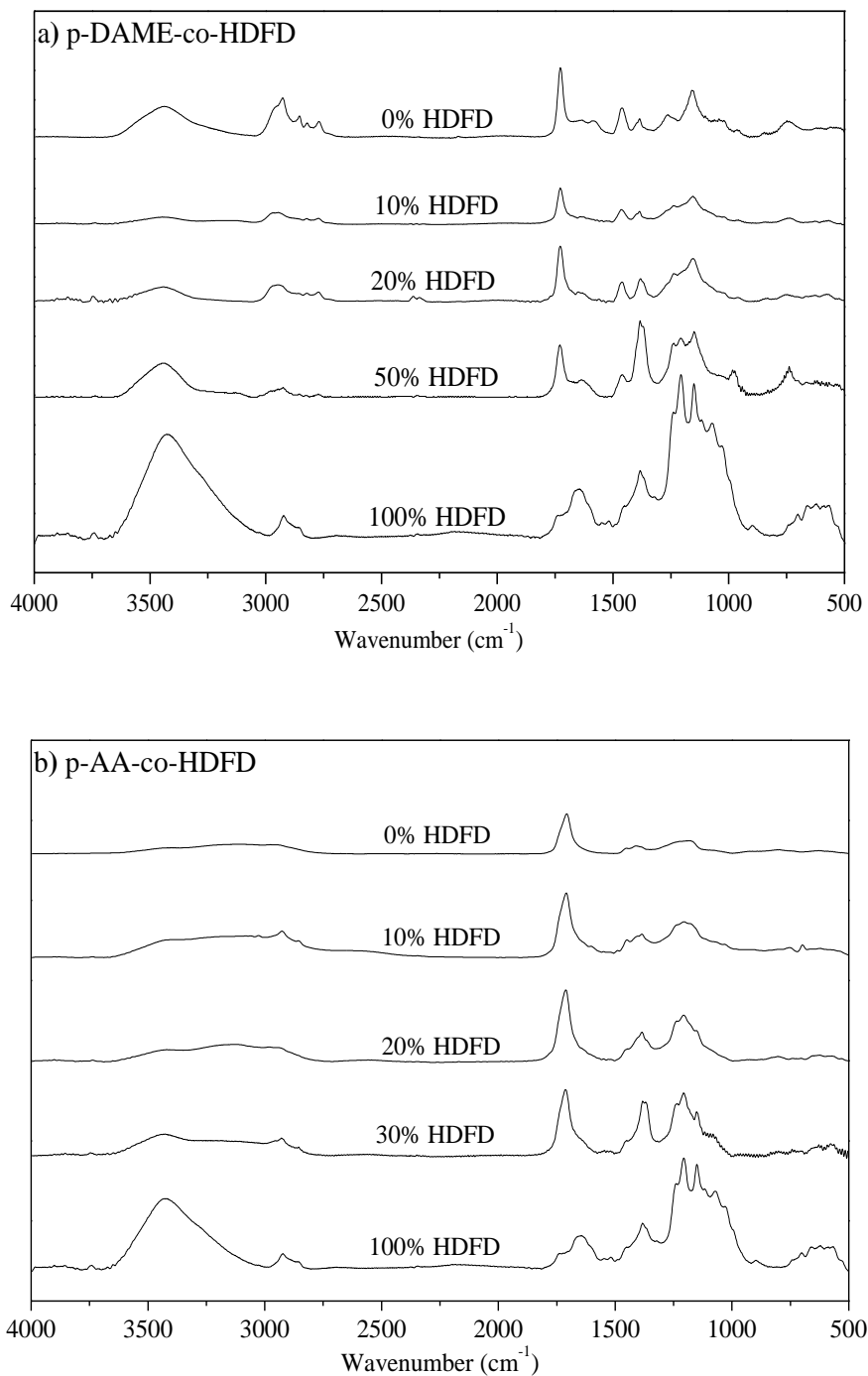


Figure 1. FTIR spectra of a) p-DAME-co-HDFD and b) p-AA-co-HDFD films according to the HDFD proportion ($P = 10\text{W}$, $f = 6\text{ kHz}$, $d.c. = 10\%$, $t = 10\text{ min}$).

To investigate the changes in surface composition as a function of HDFD proportion, XPS was performed on PC films coated with p-DAME-co-HDFD or p-AA-co-HDFD (**Figure 2**). The different co-deposits contain the elements of each homopolymer as also noticed with FTIR analyses. The detected oxygen (12 %) in p-HDFD surface may be due to the post-

oxidation or to the recombination between trapped free radicals in p-HDFD and PC substrate fragments created in the plasma phase after its Ar plasma pre-treatment. Nitrogen is present in a low concentration in the different p-DAME-co-HDFD coatings and also in p-DAME (4.4 to 5.4 % and 6.5 % respectively). When the HDFD percentage increases in the plasma mixture, the amount of fluorine in p-DAME-co-HDFD and p-AA-co-HDFD coatings also increases while the amount of O and / or N decreases. This means that the layers tend to be more hydrophobic. This observation is confirmed by the rise of the $F / (O + N)$ ratio ($N = 0\%$ in the case of p-AA-co-HDFD) HDFD proportion (**Table 2**).

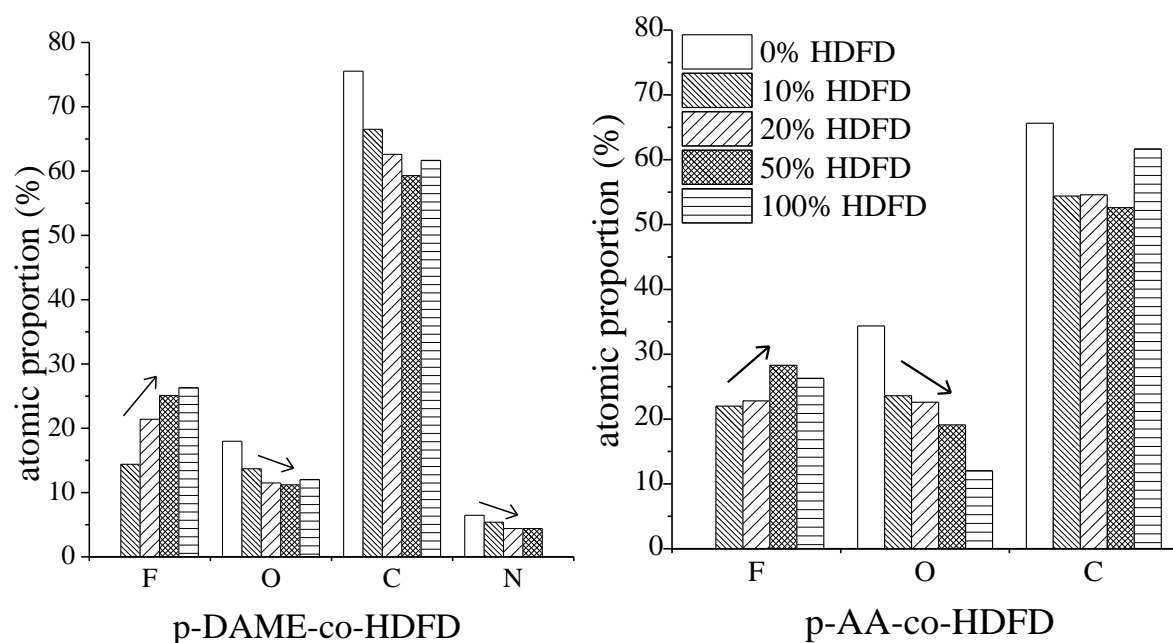


Figure 2. Dependence of the atomic F, C, O, N percentages (XPS data) in (co)polymers on the HDFD concentration in the plasma phase ($P = 10\text{ W}$, $f = 6\text{ kHz}$, $d.c. = 10\%$, $t = 10\text{ min}$).

To further investigate the dependence of the alterations in the surface chemistry on the HDFD proportion, high resolution C1s XPS spectra were also recorded and illustrated with 20 % of HDFD in the plasma phase (**Figure 3** and **Table 2**).

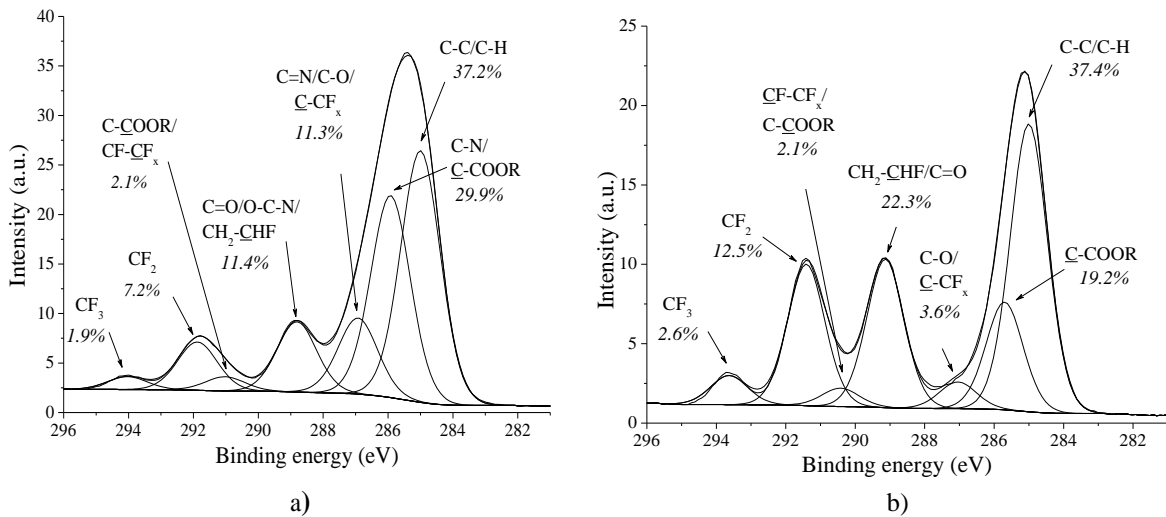


Figure 3. High resolution C1s spectra of a) p-DAME-co-HDFD, and b) p-AA-co-HDFD ([HDFD] = 20 %, $P = 10$ W, $f = 6$ kHz, $d.c. = 10$ %, $t = 10$ min).

Table 2. Proportion of CF_2 , CF_3 , (\underline{C} -COOR + C-N) groups and $F / (O + N)$, CF_2 / CF_3 , $(CF_2 + CF_3) / (\underline{C}$ -COOR + C-N) groups ratio from XPS data in plasma co-deposits as a function of different [HDFD] ($P = 10$ W, $f = 6$ kHz, $d.c. = 10$ %, $t = 10$ min).

| | % HDFD | F / (O + N) | CF_2 | CF_3 | \underline{C} -COOR, C-N | CF_2 / CF_3 | $(CF_2 + CF_3) / (\underline{C}$ -COOR + C-N) |
|----------------|--------|-------------|--------|--------|----------------------------|---------------|---|
| p-DAME-co-HDFD | 0 | | | | 29.9 | | |
| | 10 | 0.75 | 3.8 | 0.9 | 31.3 | 4.22 | 0.15 |
| | 20 | 1.34 | 7.2 | 1.9 | 29.9 | 3.79 | 0.30 |
| | 50 | 1.61 | 11.2 | 2.7 | 27.3 | 4.15 | 0.51 |
| | 100 | 2.18 | 13.9 | 2.7 | | 5.15 | |
| p-AA-co-HDFD | 0 | | | | 9.7 | | |
| | 10 | 0.93 | 11.4 | 2.3 | 16.7 | 4.96 | 0.82 |
| | 20 | 1.01 | 12.5 | 2.6 | 19.2 | 4.81 | 0.79 |
| | 50 | 1.48 | 18.7 | 3.8 | 14.2 | 4.92 | 1.58 |
| | 100 | 2.18 | 13.9 | 2.7 | | 5.15 | |

The C1s XPS spectra of the two co-deposits are decomposed into seven peaks relevant of carbon – oxygen or carbon – fluorine bonds as shown in **Figure 3**. The percentage of each component varies according to the relative proportion of each monomer. The increase of HDFD concentration in the gas mixture leads to the rise of CF_3 and CF_2 groups when at the same time, \underline{C} -COOR or CN species decreases. From Table 2, the $(CF_2 + CF_3) / (\underline{C}$ -COOH + CN) calculated

ratio which is representative of the hydrophobic - hydrophilic balance, increases with increasing the HDFD proportion in each mixture. Whatever the HDFD proportion, the hydrophobic part in this balance is more consequent for p-AA-co-HDFD film than in p-DAME-co-HDFD one. Compared to pure plasma phases in which AA appears to be more reactive than DAME, adding HDFD molecules in AA atmosphere induces a strong decrease of deposition rate of p-AA-co-HDFD (i.e. AA reactivity) and a less HDFD fragmentation while in DAME gas, the equivalent deposition rate slowly decreases (Table 1). Moreover, the atomic ratio of hydrophobic / hydrophilic functional group depends also on the proportion of their initial precursor. For the same proportion in the mixture, the ratio of ($\text{CF}_2 + \text{CF}_3$) of HDFD ($\text{C}_{10}\text{H}_3\text{F}_{13}$) with DAME ($\text{C}_8\text{H}_{15}\text{NO}_2$) is always lower than with AA ($\text{C}_3\text{H}_4\text{O}_2$). Therefore, the p-AA-co-HDFD is more fluorinated.

Moreover, since each hydrophobic chain contains only one terminal trifluorocarbon, the length of the fluorinated chain can be accessed from the ratio of difluorocarbon to trifluorocarbon.^[21] This ratio for all co-deposits and for p-HDFD (< 5.15) is lower than that of HDFD monomer ($= 7$) indicating the presence of scission, fragmentation of the precursor molecule. According to^[24] and^[25], hydrogen addition in plasma phase favors the polymerization of perfluorocarbon. Due to the higher hydrogen content in the DAME structure, the polymerization of HDFD is enhanced. In other words, the perfluorocarbon chains of HDFD are more fragmented then shorter with the presence of DAME in the mixture, compared to that of AA. For each HDFD proportion, the $\text{CF}_2 / \text{CF}_3$ ratios are more important in the acrylic-based co-deposits (4.81 - 4.96) than in the amino-based co-deposits (3.79 - 4.15), meaning that the perfluorocarbon chains are more preserved and longer in the former than in the latter material.

In conclusion, the increase of the hydrophobic component in p-DAME-co-HDFD and p-AA-co-HDFD with the raise of HDFD proportion in the mixture has been demonstrated by the increase of $\text{F} / (\text{O} + \text{N})$ and $(\text{CF}_2 + \text{CF}_3) / (\text{C-COOR} + \text{C-N})$ ratios from XPS data. Moreover, whatever the plasma conditions of the co-deposits, the fluorinated chains length of both films

seems to be independent on [HDFD] in the plasma phase but, the fluorinated chains of p-AA-co-HDFD are longer than that of p-DAME-co-HDFD.

3.2 Antifogging property of hydrophilic / oleophobic plasma co-deposits

In this part, the wetting behavior with water (or hexadecane) and the anti-fogging property of the various plasma-co-deposits are examined in connection with their chemical composition.

3.2.1 Influence of the chemical composition of the plasma phase on the layer wettability

Surface properties of the different co-deposits from DAME / HDFD and AA / HDFD prepared with various HDFD concentrations from 10 - 80 % at $P = 10 \text{ W}$, $d.c. = 10 \%$, $f = 6 \text{ kHz}$, $t = 10 \text{ min}$ can also arise from the wettability or contact angles measures (**Figure 4**). Homopoly(HDFD) has a hydrophobic / oleophobic surface with $WCA = 107.0 \pm 1.7^\circ$ and $HCA = 70.0 \pm 0.6^\circ$ while the p-DAME and p-AA are superhydrophilic since the water drop completely spreads on the deposit. Their respective co-deposition in the HDFD proportion $\leq 70 \%$ in the plasma phase leads to films showing the properties issued from both homopolymers : hydrophilicity with low $WCA < 20^\circ$ and oleophobicity with HCA around 70° . More precisely, the water contact angle for all acrylic acid co-deposits whatever the HDFD concentration ($WCA < 5^\circ$) is lower than that of amino-acrylate co-deposits ($WCA \leq 20^\circ$). Hydrophilic property of both co-deposits significantly decreases if the HDFD concentration in the mixture is equal to 80 % ; in such a plasma composition the WCA are $59 \pm 1.6^\circ$ and $76.6 \pm 1.3^\circ$ for p-DAME-co-HDFD and p-AA-co-HDFD respectively. It must be also noticed that the oleophobic property of p-DAME-co-HDFD outlined by HCA measure are always lower ($57.5^\circ - 64.7^\circ$) than their corresponding p-AA-co-HDFD ($69.7^\circ - 72.0^\circ$). This has to be related to lower oleophobic property due to the shorter length of the perfluorocarbon chain with DAME

coprecursor. Compared to WCA, the HCA of both co-deposits is less dependent on the HDFD proportion in the plasma phase.

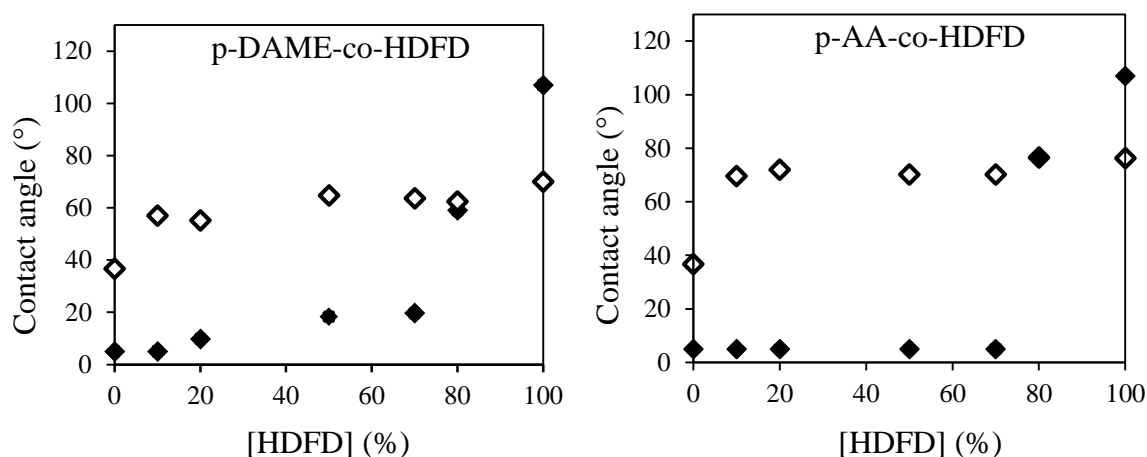


Figure 4. Dependence of the water (◆) and hexadecane (◇) contact angles, deposited on the different plasma-codeposits, versus the HDFD proportion in the plasma phase ($P = 10$ W, $f = 6$ kHz, $d.c. = 10$ %, $t = 10$ min).

In order to explain the anti-fogging properties, the literature proposed two mechanisms for hydrophilic / oleophobic surface : the first one, so-called flip-flop, is based on the rearrangement of hydrophilic segments and perfluorocarbon chains at the liquid - solid interface while the other one focuses on the water or hexadecane penetration though inter-molecular holes of the oleophobic top-layer. Dealing with the latter mechanism, the hexadecane penetration should be enhanced with a low surface fluorinated groups density and disfavoured with a high surface fluorinated groups density. As a consequence, the HCA should decrease with the increase of grafted perfluorochains density. However, for both co-deposits, the HCA and the perfluorochains length are almost constant while the surface fluorine concentration increased with the HDFD proportion (Figure 4). One may conclude that such a penetration mechanism could not be applied here and these antifogging surfaces may act as described by the formed mechanism. Thus, p-DAME-co-HDFD and p-AA-co-HDFD are anti-fogging flip-flop type.

3.2.2 Influence of the chemical composition of the plasma phase on antifogging property of the layer

Figures 5, 6 present the evolution of transmittance of the different polymeric substrates after the water vapor exposition. The dry pristine PC represents the reference. After being exposed to the water vapor, the wet pristine PC loses its transparency because of the fog formation that scatters the light and reduces the optical efficiency. Such phenomenon is reversible and the substrate recovers its initial transmittance after 3 min thanks to the water evaporation. All the synthesized layers are tested. But only p-DAME-co-HDFD and p-AA-co-HDFD synthesized with HDFD proportion $\leq 70\%$ and 60% , respectively, present such a hydrophilic / oleophobic property which allows the water adsorption due to their hydrophicity and which reduces the hydrocarbon contamination due to their oleophobicity. These wet PC coated either with hydrophilic / oleophobic p-DAME-co-HDFD or p-AA-co-HDFD remain transparent without any fog formation. After more than 3 min, the adsorbed water begins to evaporate and the transmittance of the different coated PC tends to the value of the dry pristine substrate. So the prepared layers are anti-fogging and anti- airborne hydrocarbon contamination materials.

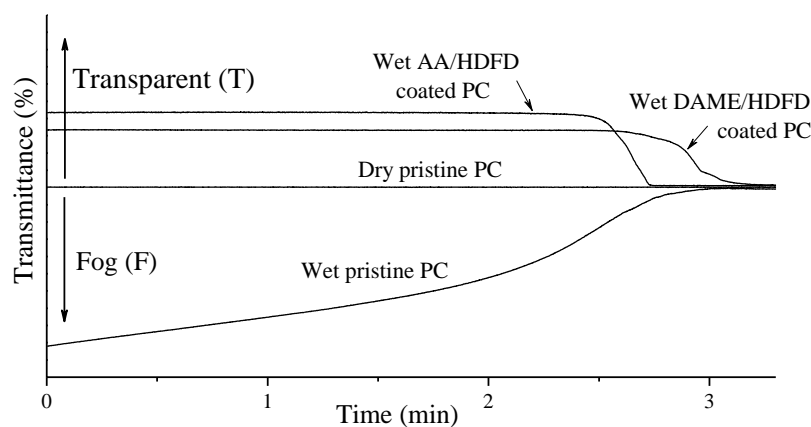


Figure 5. Light transmission ($\lambda = 550 \text{ nm}$) over time through the dry, wet pristine and coated PC : p-DAME-co-HDFD, p-AA-co-HDFD exposed 1 min to the water vapor ($[\text{HDFD}] = 20\%$, $P = 10 \text{ W}$, $f = 6 \text{ kHz}$, $d.c. = 10\%$, $t = 10 \text{ min}$).

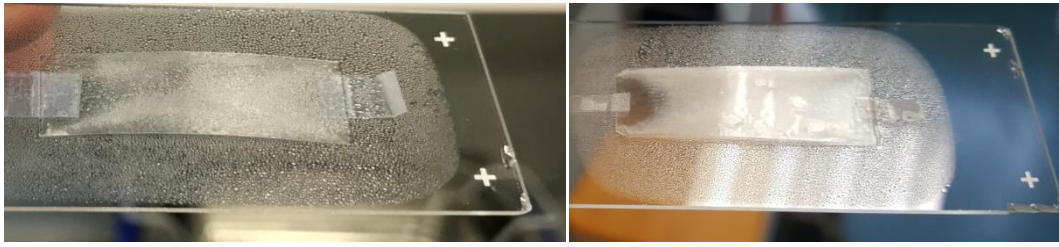


Figure 6. Illustration of antifogging results of wet pristine (left) and wet coated PC (p-AA-co-HDFD : [HDFD] = 20 % , $P = 10$ W, $f = 6$ kHz, $d.c. = 10$ %) (right) exposed 1 min to the water vapor.

The outline of the chemical composition, the wettability and the anti-fogging property of the different synthesized layers is summarized in **Table 3**. Due to their hydrophilicity, p-DAME and p-AA show anti-fogging properties. On the contrary, p-HDFD leads to fog formation due to its hydrophobicity. When the HDFD proportion is comprised between 10 % to 70 % in DAME / HDFD mixture or 10 % to 60 % in AA / HDFD mixture, the obtained co-deposits are hydrophilic, oleophobic and also anti-fogging. If the HDFD concentration in the plasma phase is equal to 80 %, the anti-fogging properties of p-DAME-co-HDFD and p-AA-co-HDFD are lost since the films are no more hydrophilic. Surprisingly, the anti-fogging property of p-AA-co-HDFD is lost when the HDFD proportion is 70 % even if the contact angle criteria are respected (i.e. $WCA < 20^\circ$ and HCA close to 70°). Such unexpected result showing data inconsistency could be explained by the difference of the contact area between the water drop used for contact angle measurements and that one developed during the water vapor test, the latter one being much smaller and able to detect hydrophobic area hidden (or underestimated) within the wettability measurements. Beside the chemical behavior of these antifogging coatings, their roughness and their chemical surface heterogeneity may play an important part on the wetting and antifogging properties. SEM images (not shown here) show smooth surfaces comparable before and after water vapor contact. AFM images cannot be performed because of the initial PC substrate roughness. Works are under progress for preparing PC substrate as smooth as possible.

Table 3. Properties of the different synthesized co-deposits versus HDFD concentration in the plasma phase

| p-DAME-coHDFD | | | |
|---------------|-------------|--------------------------|-------------|
| [HDFD] (%) | 0 | 10 - 70 | ≥ 80 |
| Wettability | Hydrophilic | Hydrophilic - Oleophobic | Hydrophobic |
| Antifogging | | Antifogging | Fogging |
| p-AA-co-HDFD | | | |
| [HDFD] (%) | 0 | 10 - 60 | 70 |
| Wettability | Hydrophilic | Hydrophilic - Oleophobic | Hydrophobic |
| Antifogging | | Antifogging | Fogging |

* proportion in the plasma phase

4 Conclusion

Simultaneously hydrophilic / oleophobic p-DAME-co-HDFD or p-AA-co-HDFD were deposited on PC substrate by using the pulsed plasma chemistry. Increasing the HDFD proportion in gas mixture enhances the hydrophobicity but does not alter the oleophobicity of the surface. We assumed that the p-AA-co-HDFD is more oleophobic than the p-DAME-co-HDFD due to their longer fluorocarbon chains whatever the HDFD proportion. These layers synthesized with a HDFD proportion ≤ 70 % exhibit hydrophilic - oleophobic property with low WCA (around or less than 20°) and HCA (around $52^\circ - 70^\circ$) values but just the surfaces prepared with a percentage of HDFD ≤ 70 % for p-DAME-co-HDFD and ≤ 60 % for p-AA-co-HDFD gave a positive answer to the anti-fogging test.

Acknowledgments:

The authors thank “le Fonds unique interministériel” for its financial support

References

- [1] S. J. Dain, A. K. Hoskin, C. Winder, D. P. Dingsdag, *Ophthalm. Physiol. Opt.* **1999**, *19*, 357.
- [2] J. M. Crebolder, R. B. Sloan, *Appl. Ergonomics* **2004**, *35*, 371.

- [3] T. H. Margrain, C. Owen, *Ophthal Physiol. Opt.* **1996**, *16*, 108.
- [4] J. A. Howarter, J. P. Youngblood, *Macromol. Rapid Commun.* **2008**, *29*, 455.
- [5] B. J. Briscoe, K. P. Galvin, *Solar Energy* **1991**, *46*, 191.
- [6] D. Radloff, C. Boeffel, H. W. Spiess, *Macromolecules*, **1996**, *29*, 1528.
- [7] M. Keller, M. Lenhard, U.S. Patent 5,648,441, **1997**.
- [8] Y. Oshibe, Y. Yamamoto, H. Ohmura, K. Kumazawa, U.S. Patent 5,244,935, **1993**.
- [9] Y. Yuan, R. Liu, C. Wang, J. Luo, X. Liu, *Prog. Org. Coat.* **2014**, *77*, 785.
- [10] P. Chevallier, S. Turgeon, C. Sarra-Bournet, R. Turcotte, G. Laroche, *ACS Appl. Mater. Interfaces* **2011**, *3*, 750.
- [11] X. Du, J. He, *J. Colloid Inter. Sci.* **2012**, *381(1)*, 189.
- [12] Q. Shang, Y. Zhou, *Ceramics Internat.* **2016**, *42*, 8706.
- [13] S. Xu, H. Huang, C. Wang, Z. Huang, C. Wang, *Mat. Res. Bul.* **2015**, *65*, 210.
- [14] R. Di Mundo, R. d'Agostino, F. Palumbo, *ACS Appl. Mater. Interfaces* **2014**, *6*, 17059.
- [15] G. Grosu, L. Andrzejewski, G. Veilleux, G. G. Ross, *J. Phys. D. Appl. Phys.* **2004**, *37(23)*, 3350.
- [16] R.-D. Sun, A. Nakajima, A. Fujishima, T. Watanabe, K. Hashimoto, *J. Phys. Chem. B* **2001**, *105(10)*, 1984.
- [17] Y. Wang, J. Knapp, A. Legere, J. Raney, L. Li, *RSC Adv.* **2015**, *5(39)*, 30570
- [18] A. Vaidya and M. K. Chaudhury, *J. Colloid Inter. Sci.* **2002**, *249(1)*, 235.
- [19] H. Sawada, Y. Ikematsu, T. Kawase, and Y. Hayakawa, *Langmuir* **1996**, *12(15)*, 3529.
- [20] L. Li, Y. Wang, C. Gallaschun, T. Risch, and J. Sun, *J. Mater. Chem.* **2012**, *22(33)*, 16719.
- [21] J. A. Howarter, K. L. Genson, J. P. Youngblood, *ACS Appl. Mater. Inter.* **2011**, *3*, 2022.
- [22] J. Yang, Z. Zhang, X. Xu, X. Zhu, X. Men, X. Zhou, *J. Mater. Chem.* **2012**, *22*, 2834.
- [23] Cl. Chahine, F. Poncin-Epaillard, D. Debarnot, *Plasma Process. Polym.* **2015**, *12(5)*, 493.
- [24] H. Yasuda T. Hsu, *Surf. Sci.* **1978**, *76*, 232.

[25] J. W. Coburn, H. P. Winters, *J. Vac. Sci. Technol.*, **1979**, 16 (2), 391.

